Electronic Supplementary Material (ESI) for Journal of Materials Chemistry A.

This journal is © The Royal Society of Chemistry 2022

**Supporting Information**

**On-Chip High-Energy Interdigital Micro-Supercapacitors with 3D Nanotubular Array Electrodes**

Fei Li,[‡a] Anjun Hu, [‡a] Xiaoli Zhao,[‡b] Tongwei Wu,[a] Wei Chen,[a] Tianyu Lei,[a] Yin Hu,[a] Ming Huang*[b] and Xianfu Wang*[a]

a. State Key Laboratory of Electronic Thin Film and Integrated Devices, University of Electronic Science and Technology of China, 610054 Chengdu, P.R. China. **E-mail**: xfwang87@uestc.edu.cn.

b. Institute of Fundamental and Frontier Sciences, University of Electronic Science and Technology of China, 610054 Chengdu, P.R. China. **E-mail**: xiaoming.huang694@gmail.com

‡ These authors contributed equally to this work.

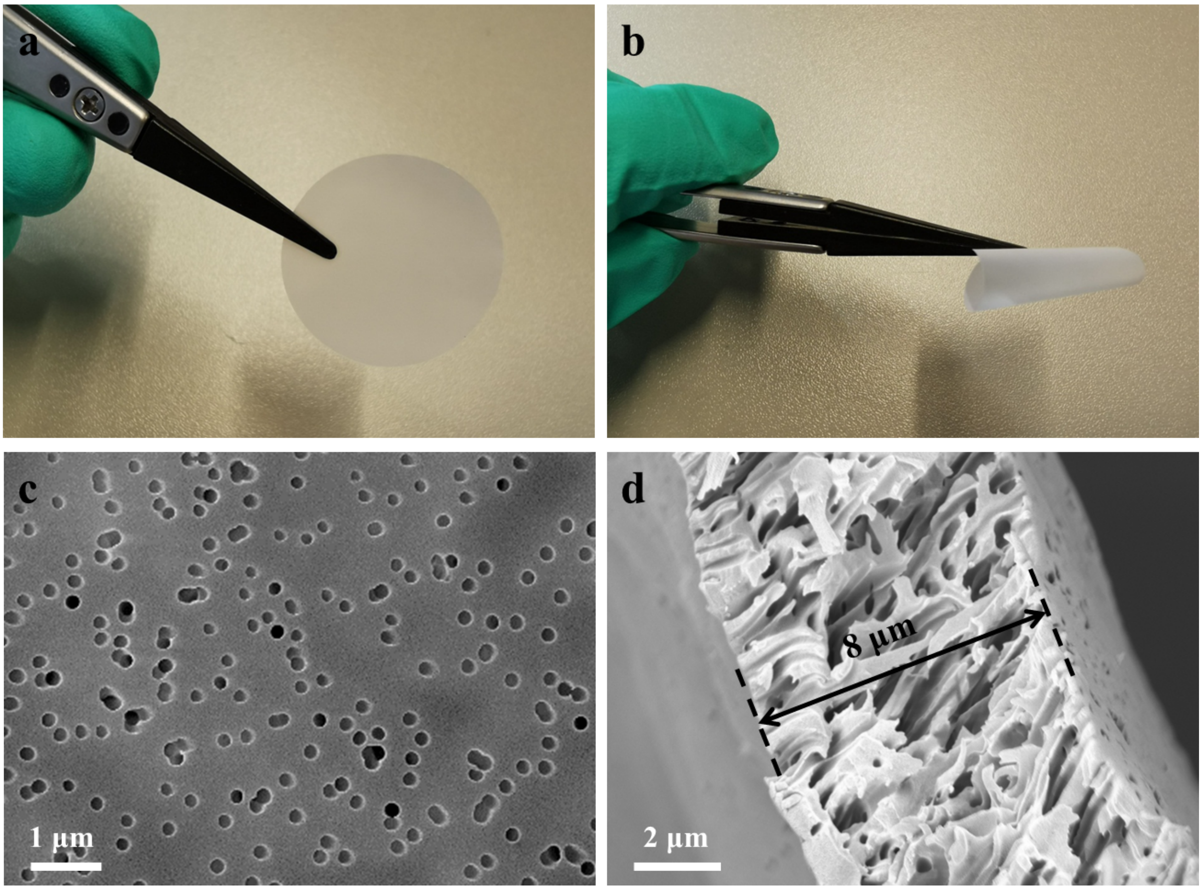


**Fig. S1**. (a, b) Photographs of polycarbonate (PC) membrane. (c, d) Top-view and cross-section SEM images of PC membrane.

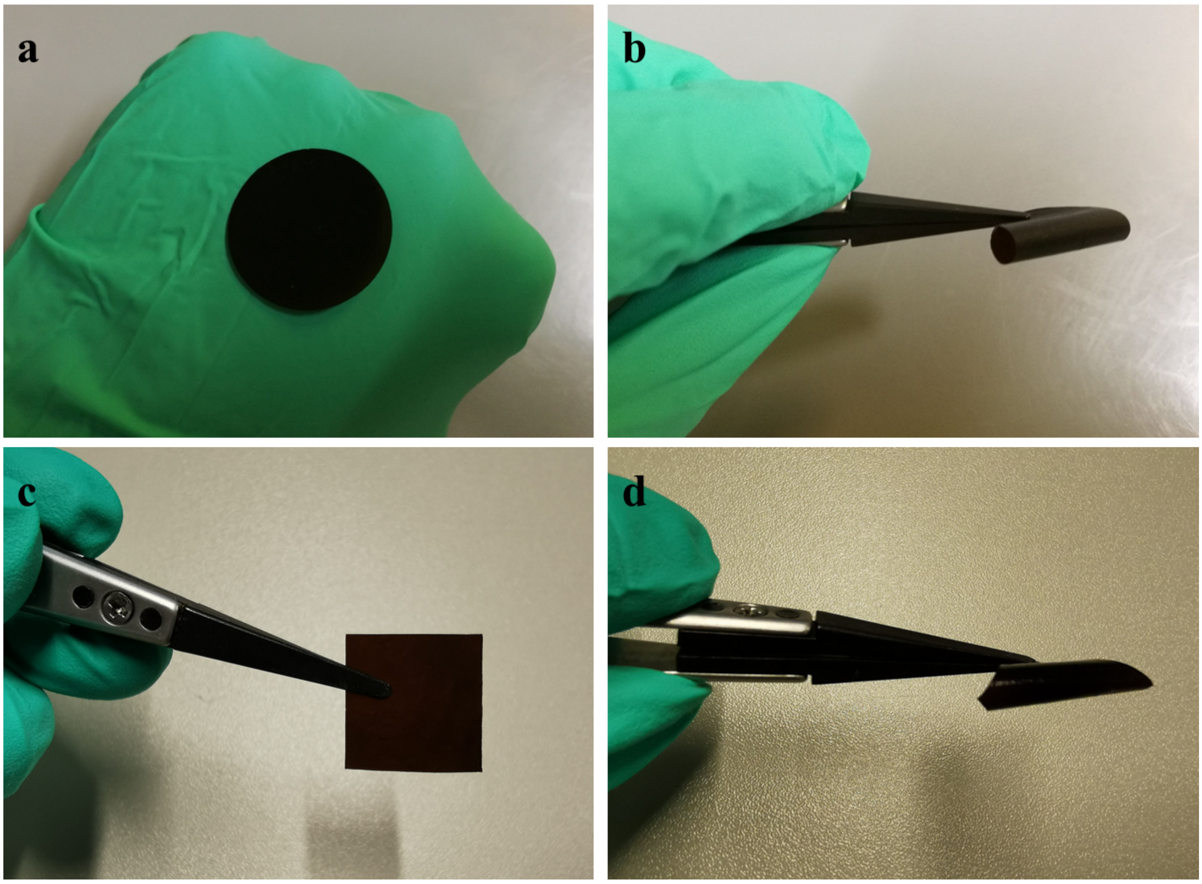


**Fig. S2**. Photographs of PC membrane after $MnO_2$ deposition at flat and bending states.

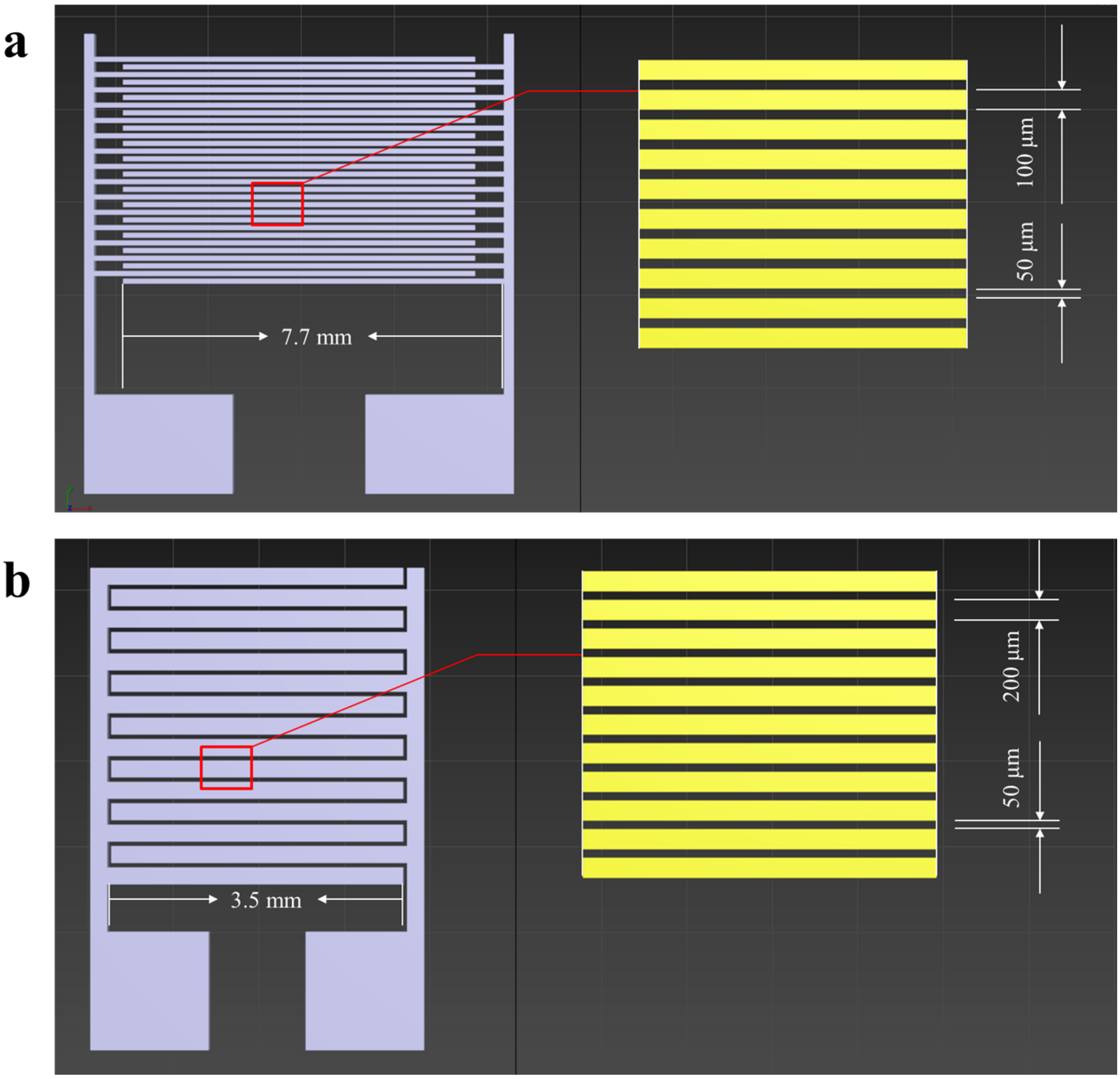


**Fig. S3.** Geometries of the MSC devices with different patterns.

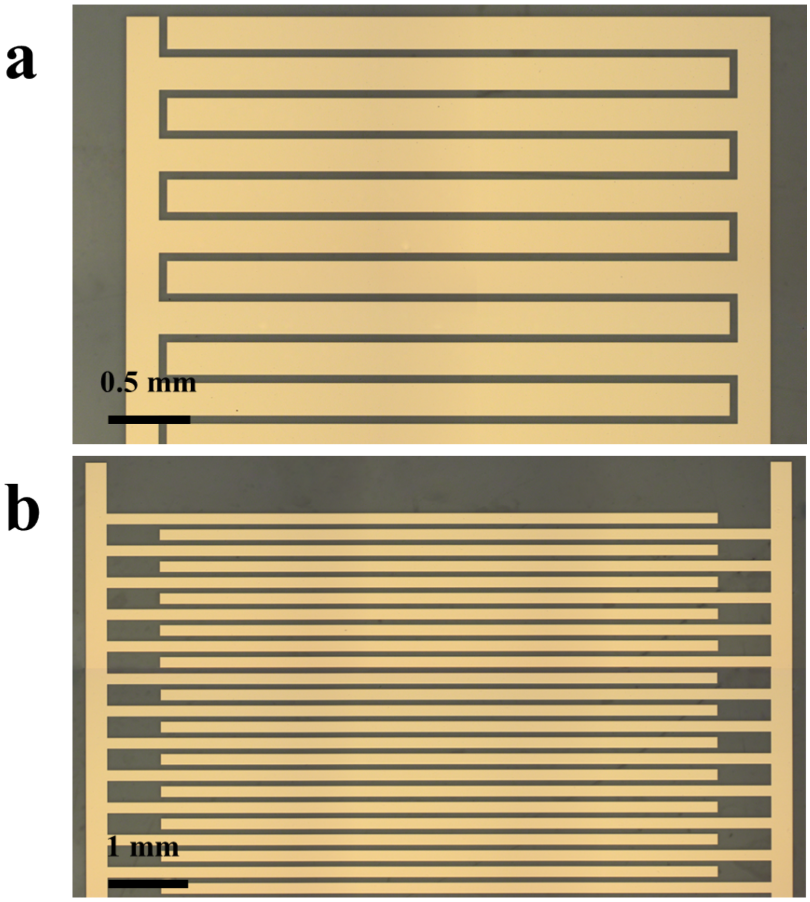


**Fig. S4**. Optical microscope images of different interdigital Cr/Au electrodes.

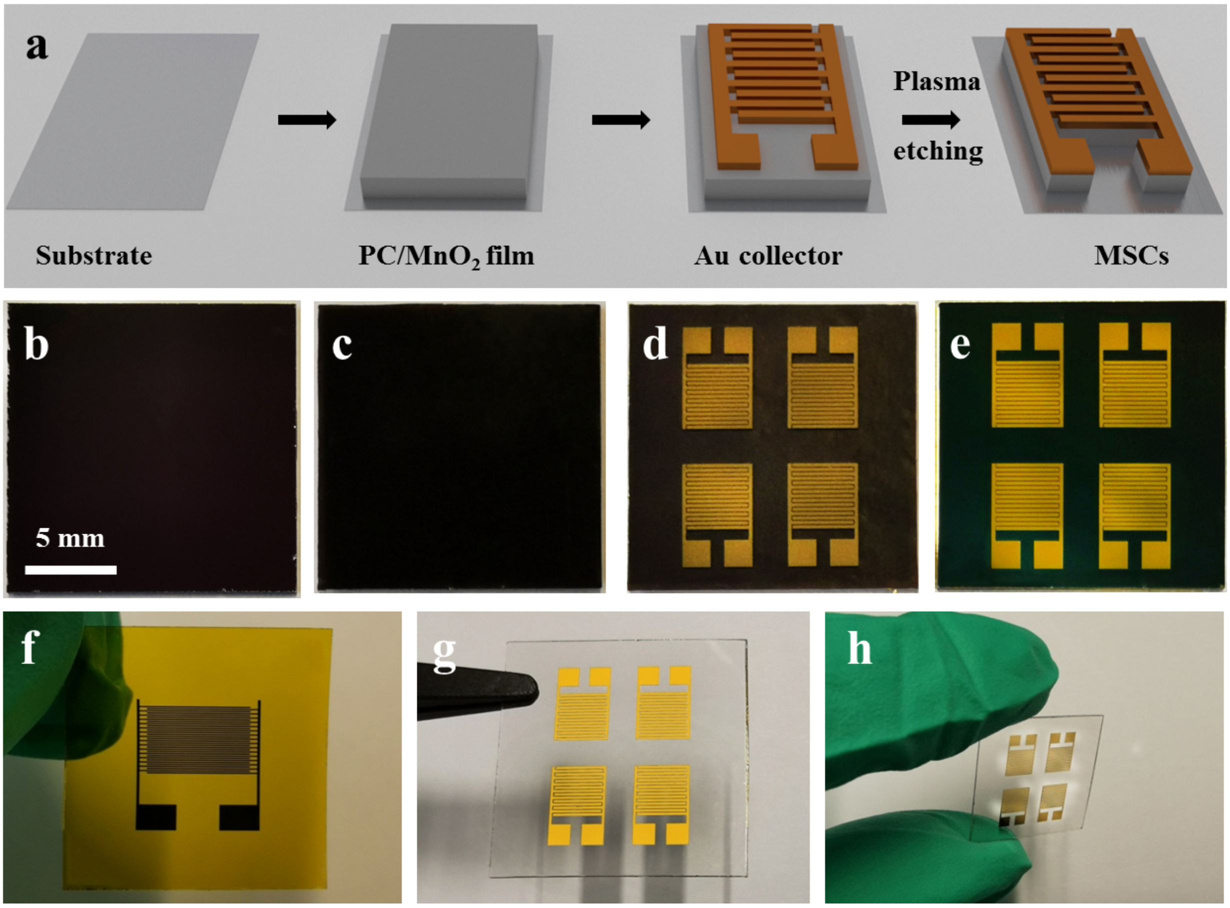


**Fig. S5**. (a) Schematic illustration showing the fabrication process of 3D MSCs. (b-e) Photographs of the device at different fabrication stages with the same size. (f-h) Photographs of 3D MSC devices with different patterns on flexible PET substrates.

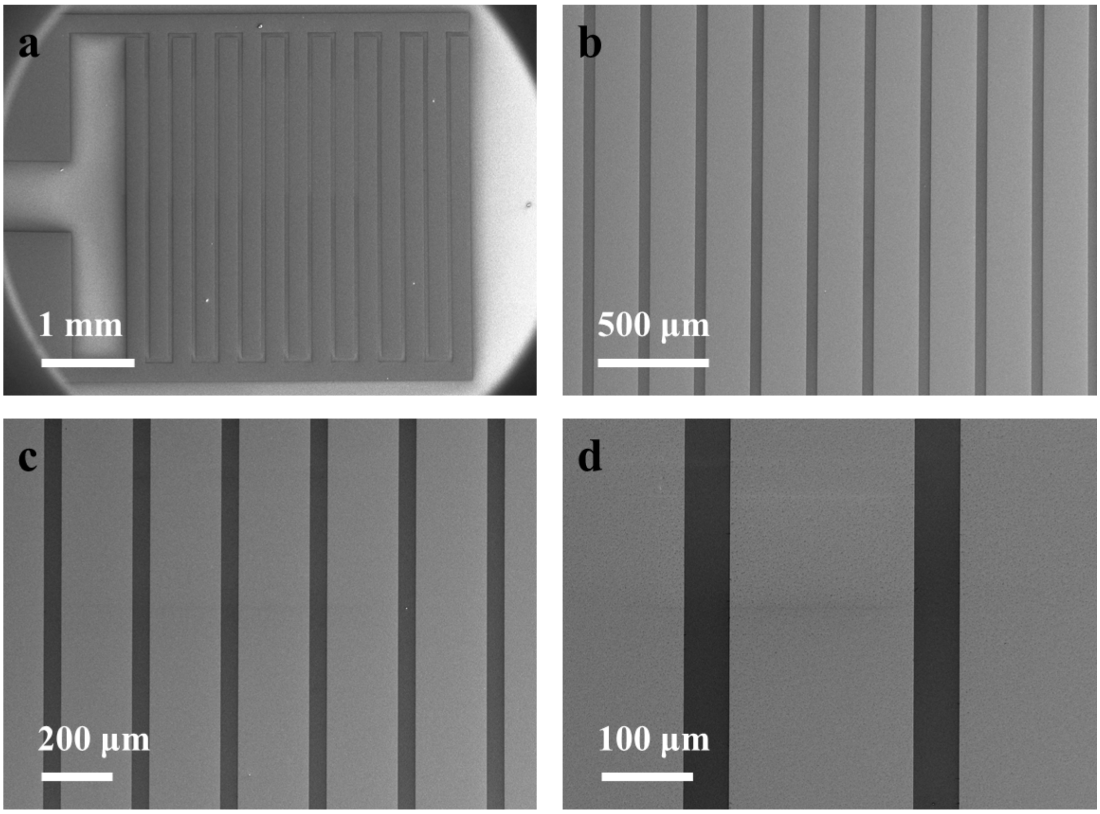


**Figure S6.** SEM images of on-chip interdigital MSCs under various magnifications.

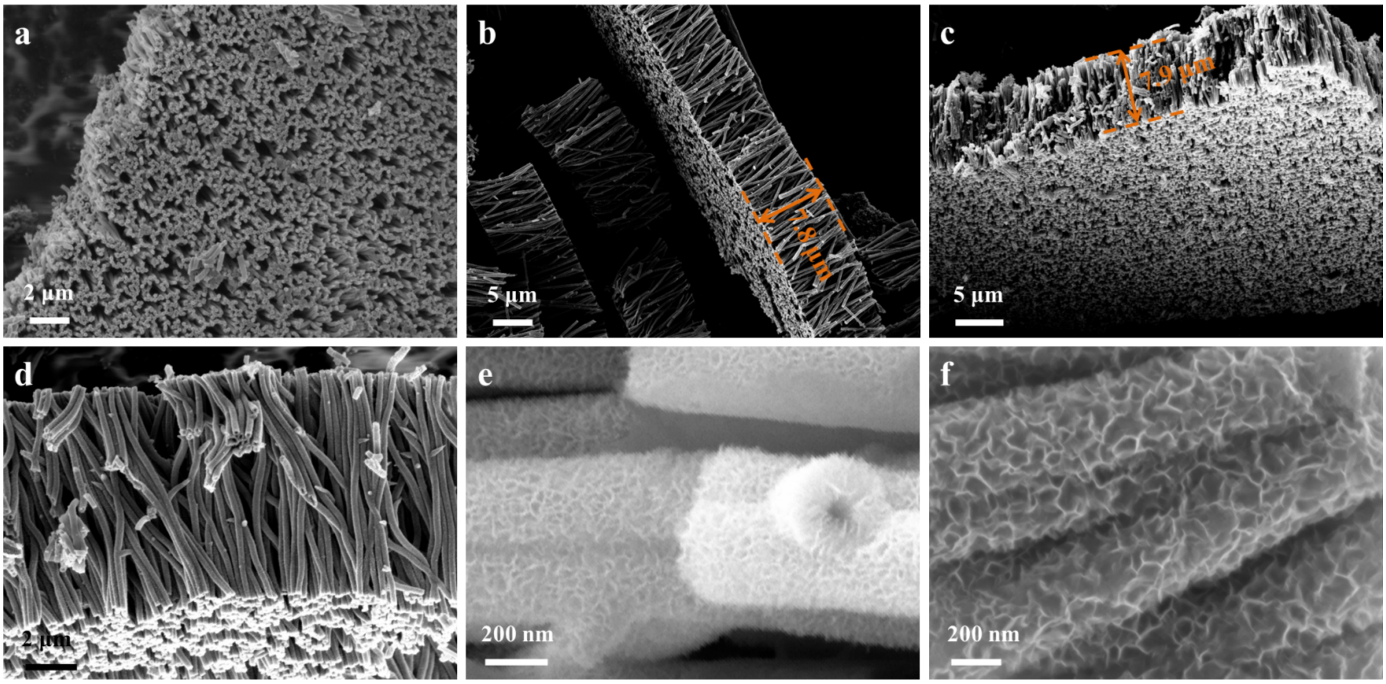


**Fig. S7**. SEM images of porous $MnO_2$ NTAs with different magnifications: (a) top-view of $MnO_2$ NTAs, (b-d) cross-section view of $MnO_2$ NTAs, and (e, f) magnified view of $MnO_2$ nanotubes.

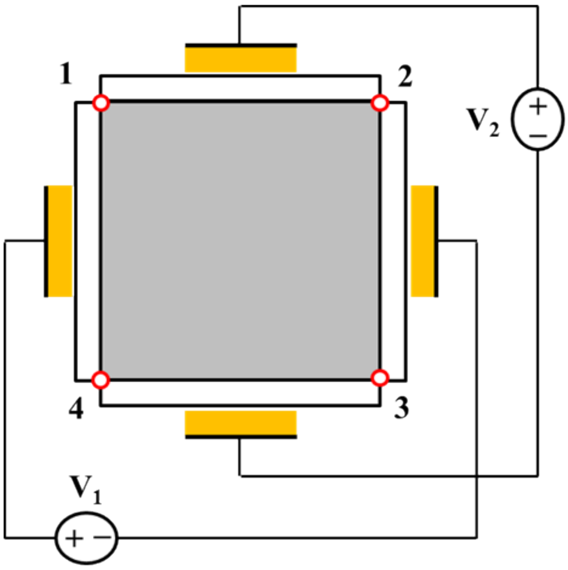


**Figure S8.** Illustration of van der Pauw technique for the conductivity measurement of $MnO_2$ NTAs film.

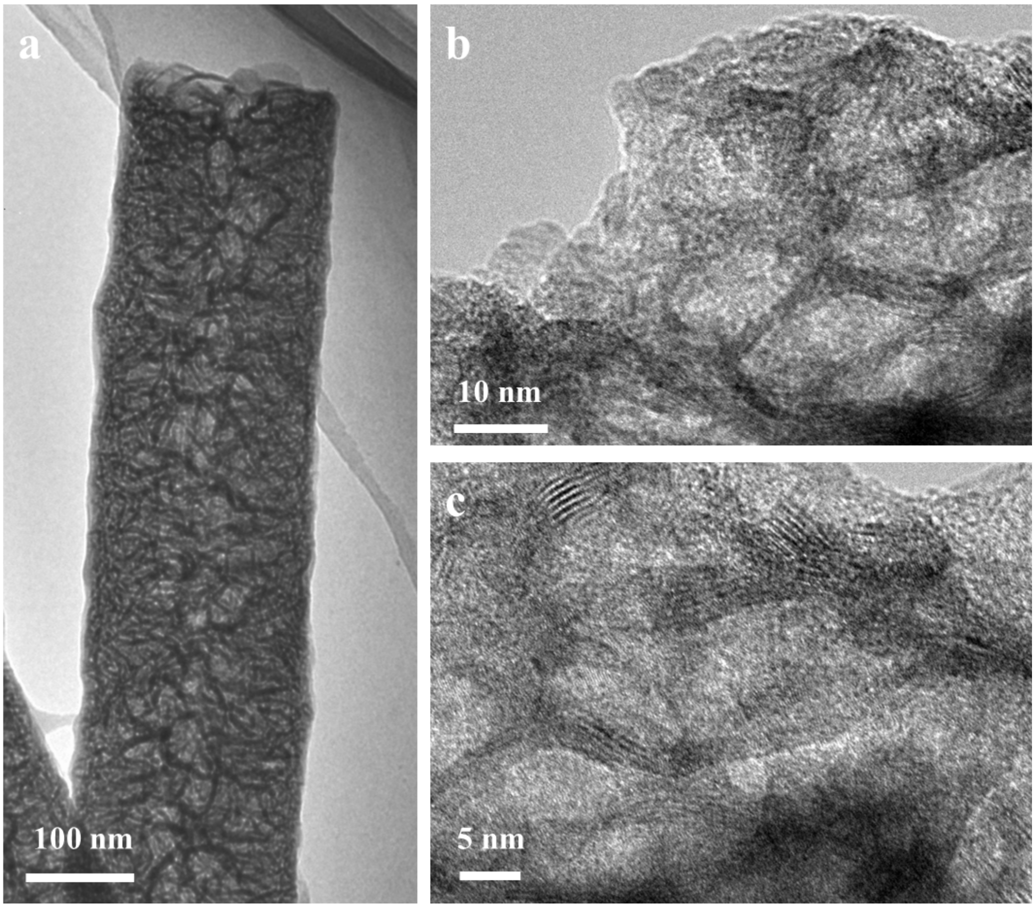


**Fig. S9**. (a) Low-magnification TEM image of an individual porous $MnO_2$ nanotube. (b, c) HRTEM images of porous $MnO_2$ nanotube.

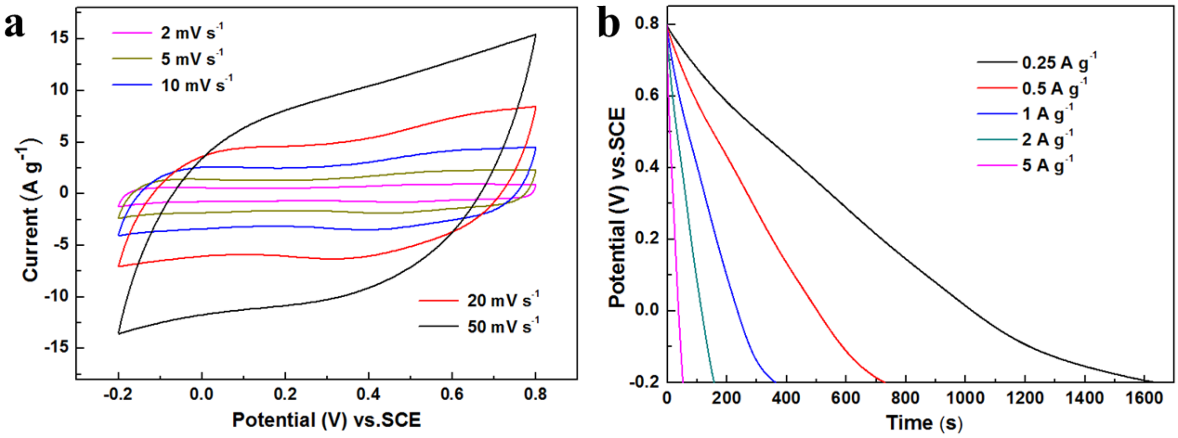


**Fig. S10**. (a) CV curves of $MnO_2$ NTAs in 1 M $Na_2SO_4$ aqueous electrolyte. (b) Discharge curves of $MnO_2$ NTAs electrode at different current densities.

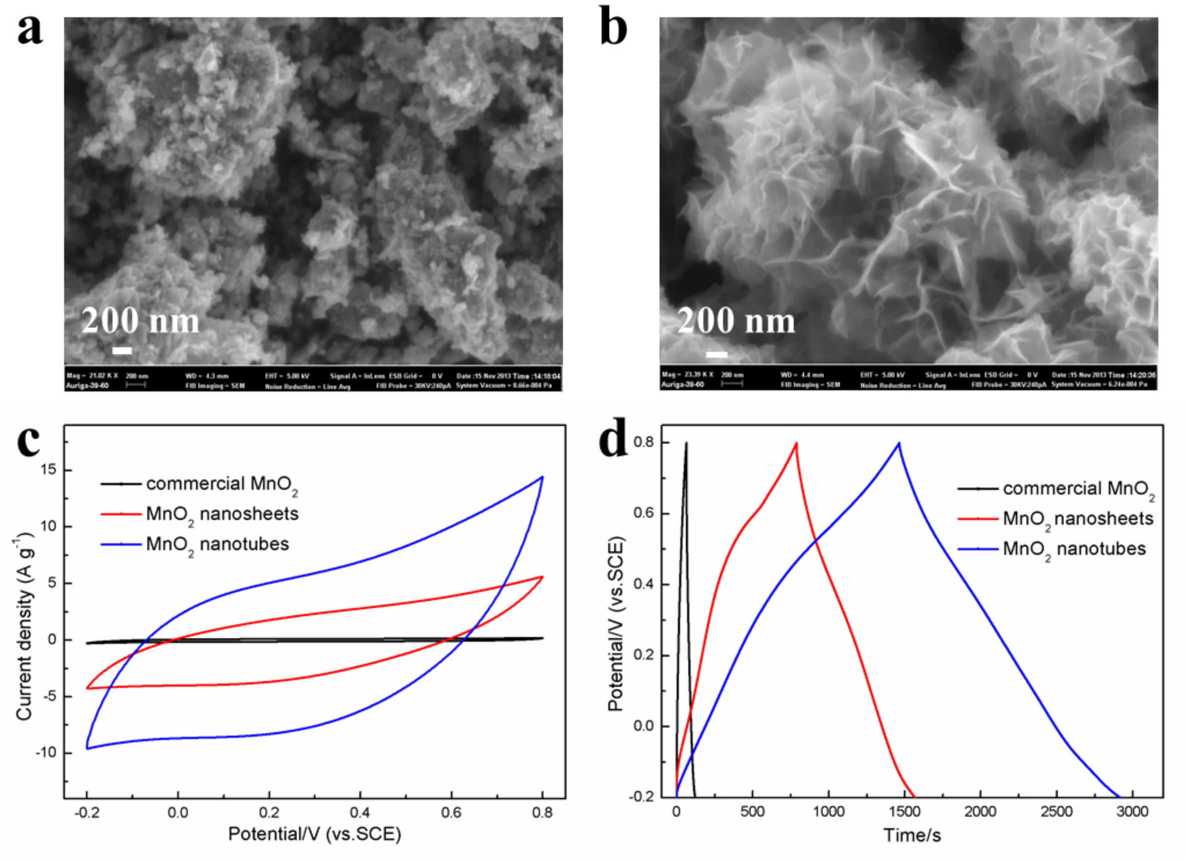


**Figure S11.** (a) SEM image of the commercial $MnO_2$. (b) SEM image of $MnO_2$ nanosheets obtained without PC template. (c) CV curves of the commercial $MnO_2$, $MnO_2$ nanosheets, and $MnO_2$ NTAs at a scan rate of 50 mV $s^{-1}$ in 1 M $Na_2SO_4$ aqueous electrolyte. (d) charge/discharge curves of the three samples at a current density of 0.25 A $g^{-1}$.

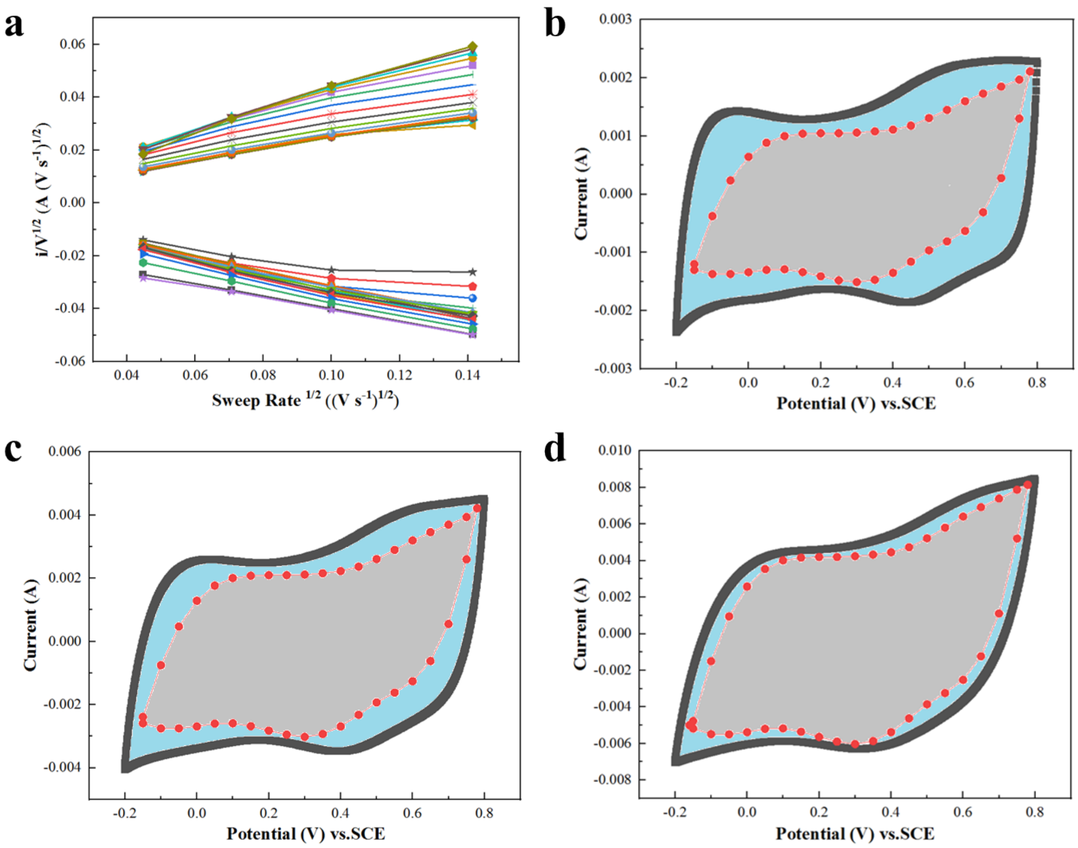


**Figure S12.** (a) Analytics of the voltammetric sweep data for $MnO_2$ NTAs electrode, sweep rates varied from 2 to 20 mV·s$^{-1}$. (b-d) CV curves of the electrode with grey shadowed area representing the surface capacitive contribution at: (b) 5 mV·s$^{-1}$; (b) 10 mV·s$^{-1}$; (c) 20 mV·s$^{-1}$.

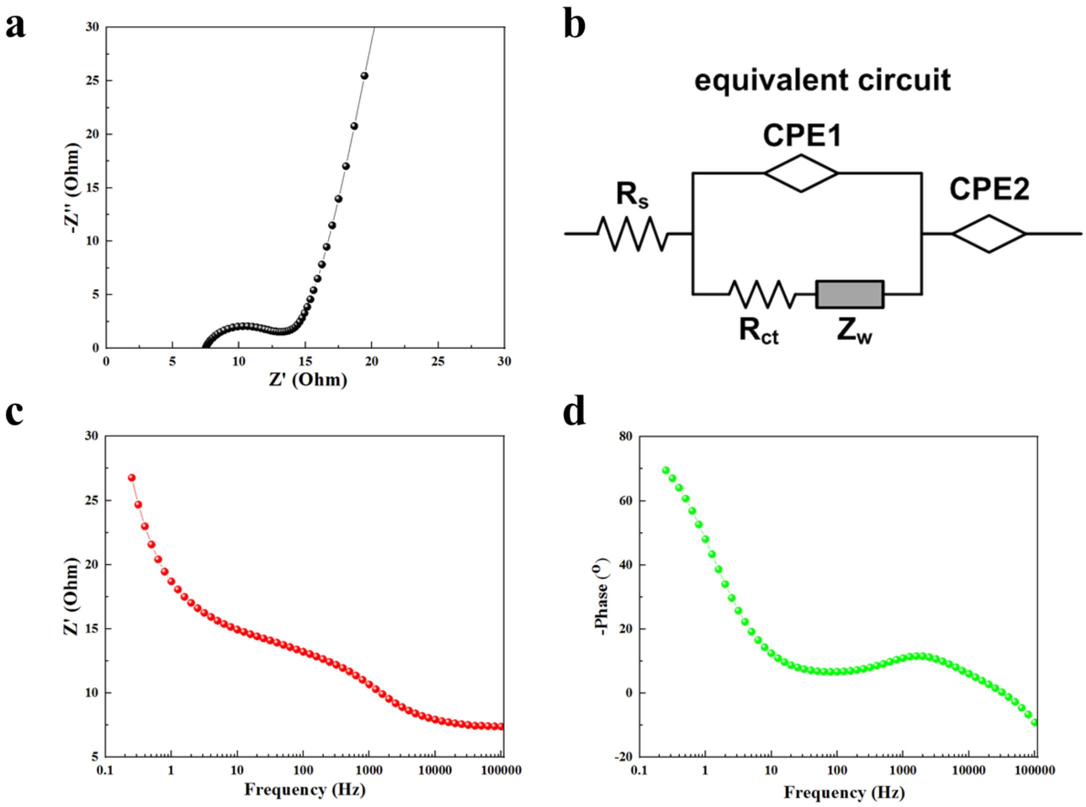


**Figure S13.** (a) Electrochemical impedance spectrum at open circuit potential in the frequency range from 0.01 Hz to 100 kHz. (d) Equivalent circuit model. (c,d) Corresponding Bode modulus and Bode phase plots.

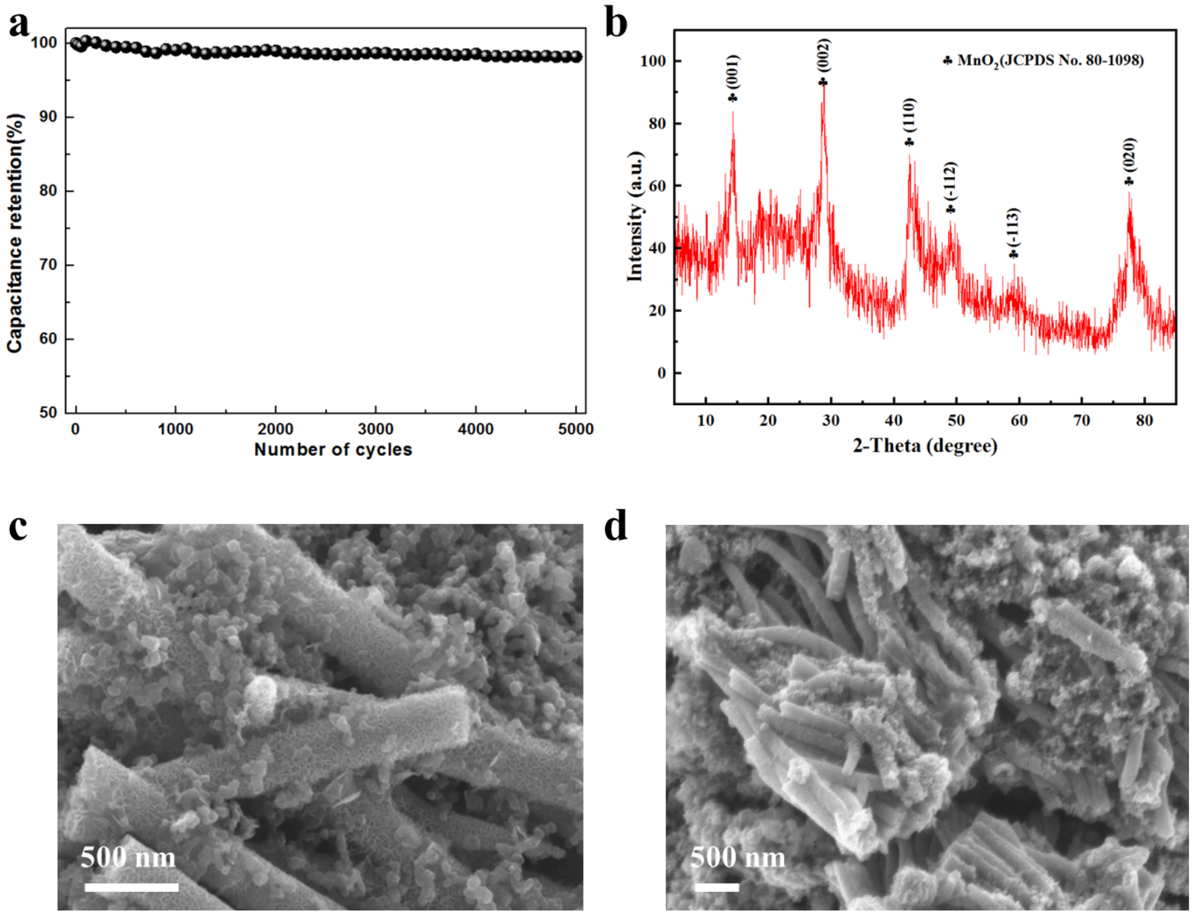


**Figure S14.** (a) Long-term cycling stability of $MnO_2$ NTAs electrode. (b) XRD pattern of the $MnO_2$ NTAs after 5000 cycles. (c,d) SEM images of $MnO_2$ NTAs electrode before and after cycling test.

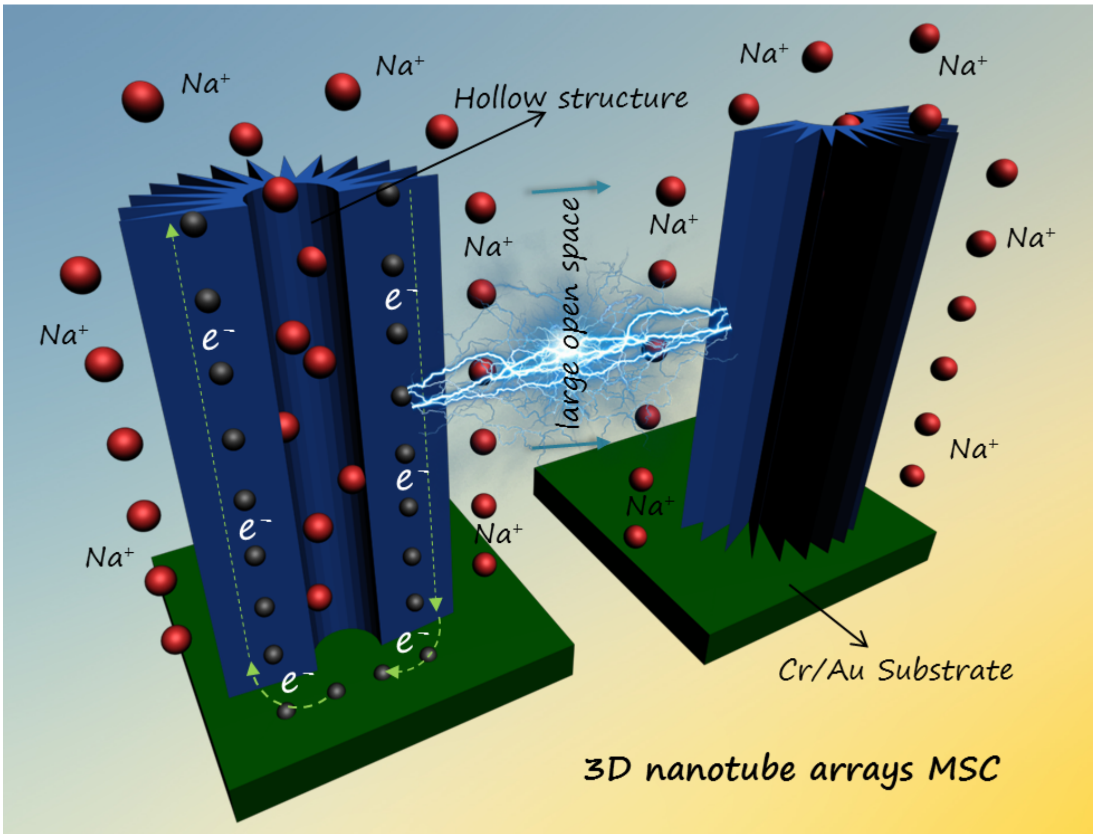


**Fig. S15**. Schematic illustration of the diffusion and transport of ions and electrons in the $MnO_2$ NTAs electrode during charge-discharge process.

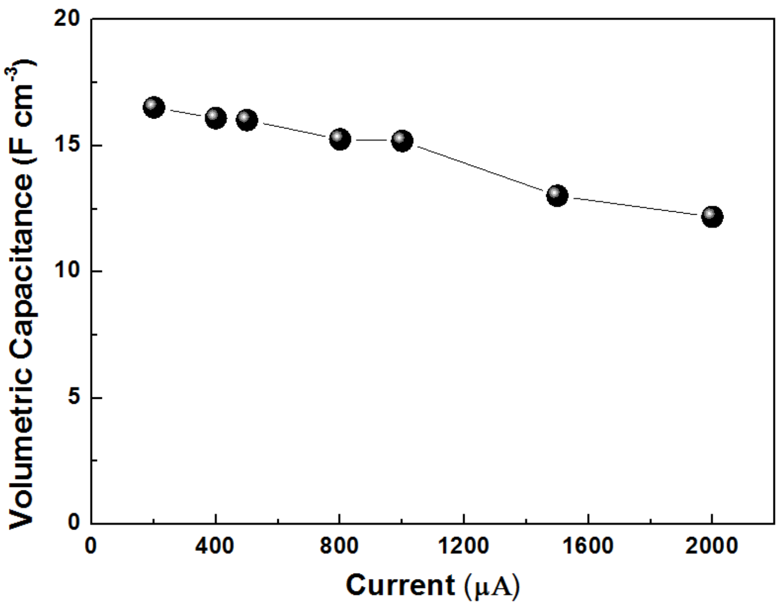


**Fig. S16**. Specific volumetric capacitance at different currents.

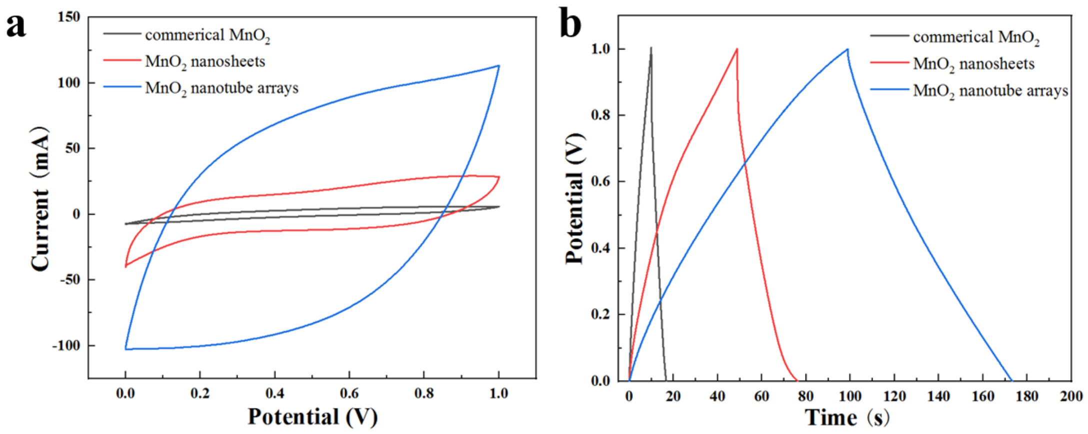


**Figure S17.** CV curves of the 3D MSC of $MnO_2$ NTAs, 2D MSC of commercial $MnO_2$ and 2D MSC of $MnO_2$ nanosheets at a scan rate of 100 mV $s^{-1}$. (d) Charge/discharge curves of the three samples at a current density of 200 μA.

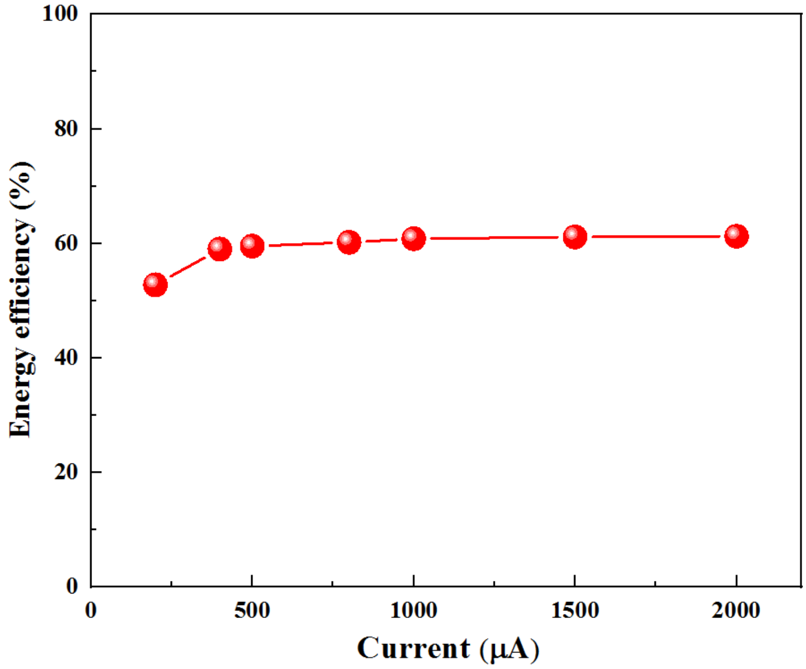


**Figure S18.** Plot of the energy efficiency with current for the 3D MSC device.

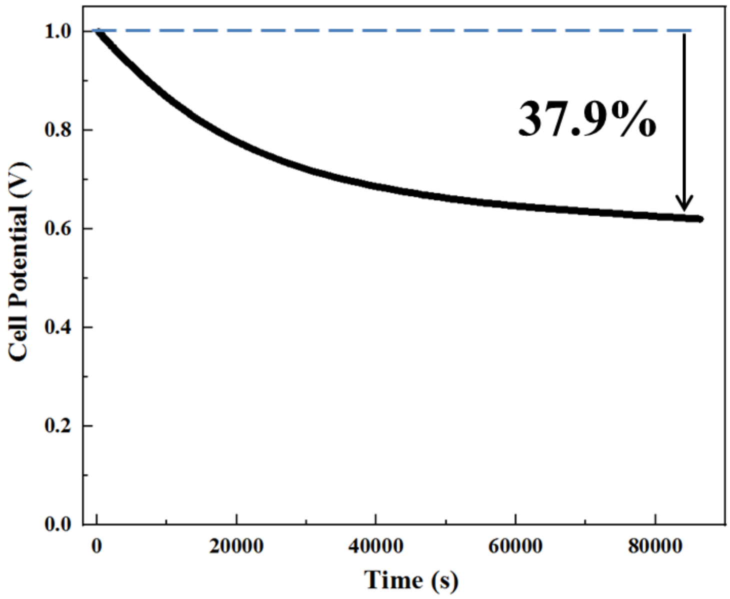


**Figure S19.** Open circuit potential decays of the 3D MSCs.

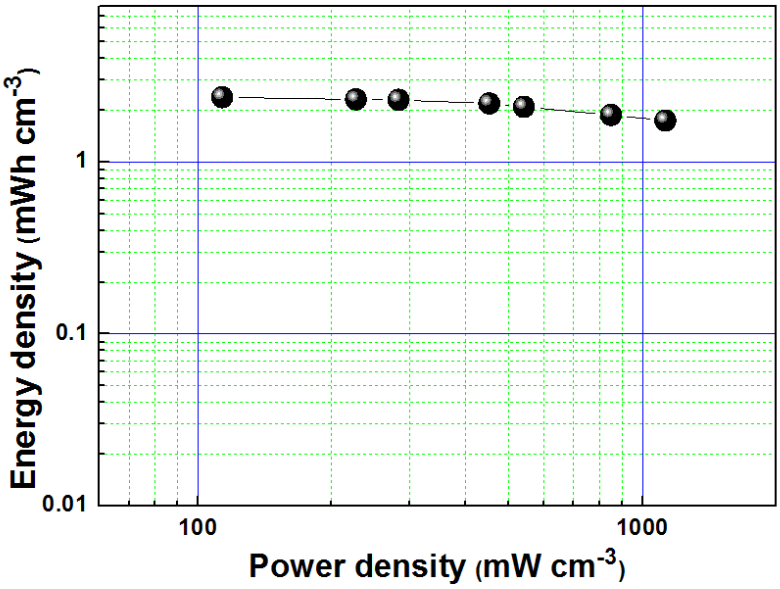


**Fig. S20.** Ragone plot of 3D $MnO_2$ NTAs-based MSCs.

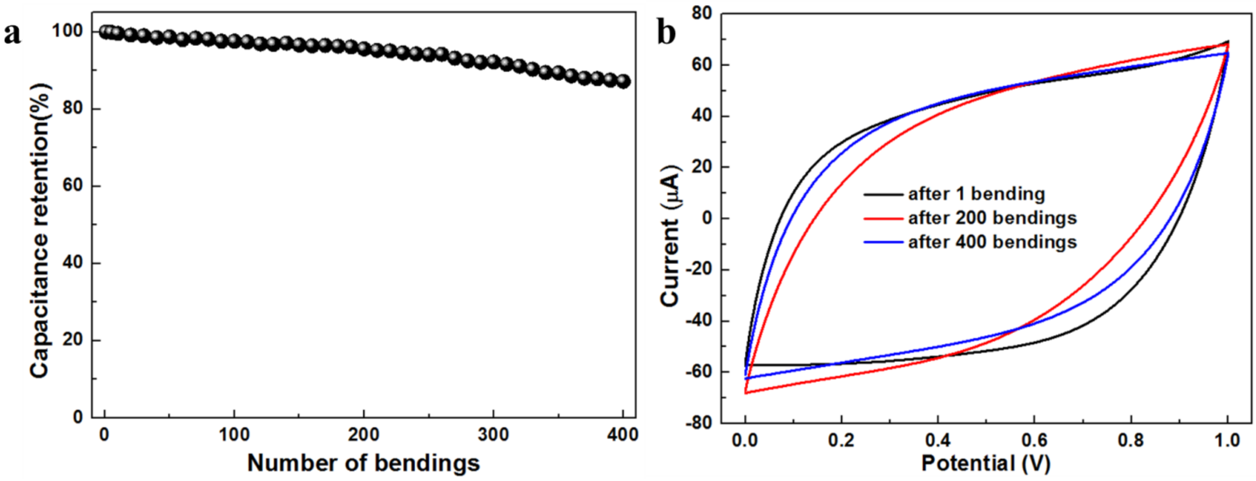


**Fig. S21**. (a) Capacitance retention as a function of bending cycle numbers. (b) Representative CV curves after different bending cycles.

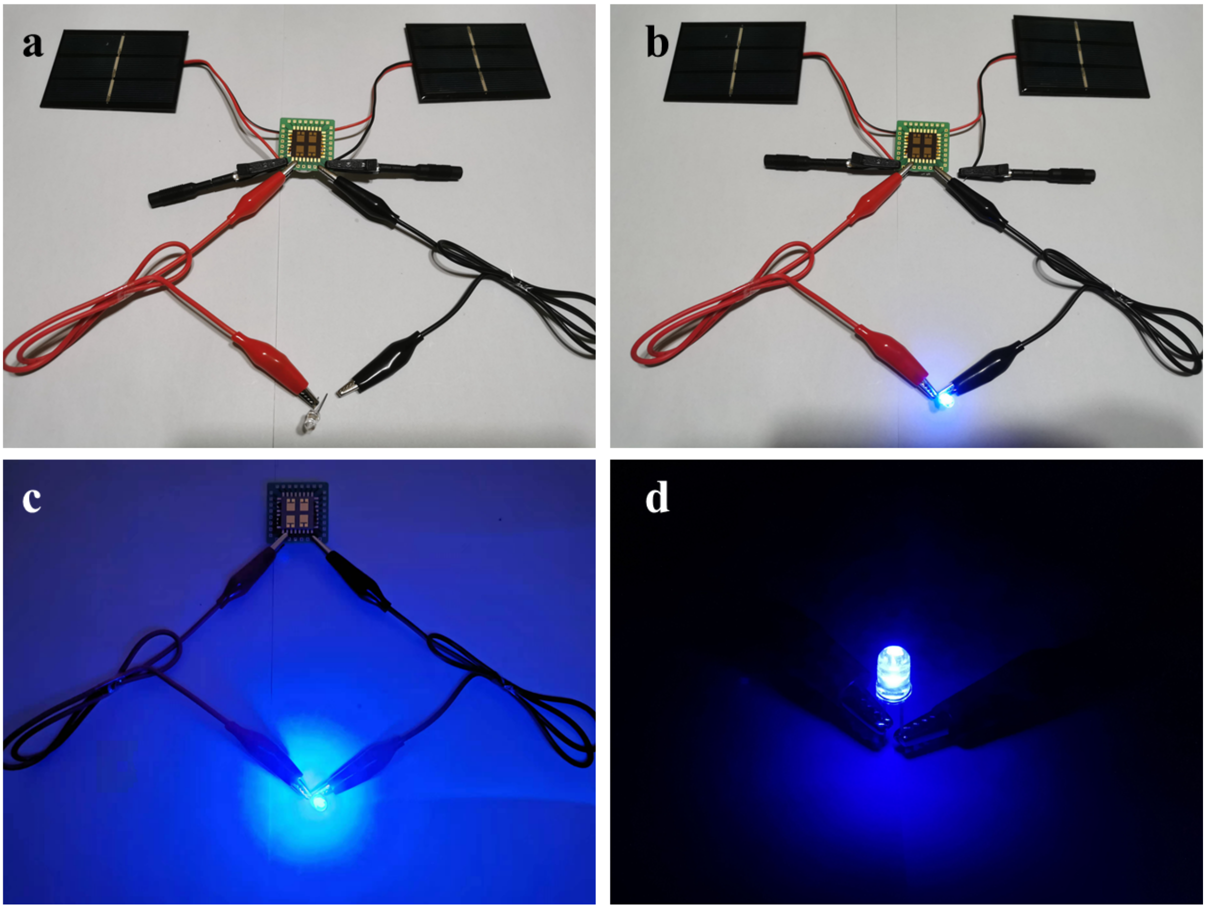


**Fig. S22**. (a, b) Photographs of the practical circuit with MSCs, solar cells and a LED. (c, d) A LED was lightened by the charged MSCs.

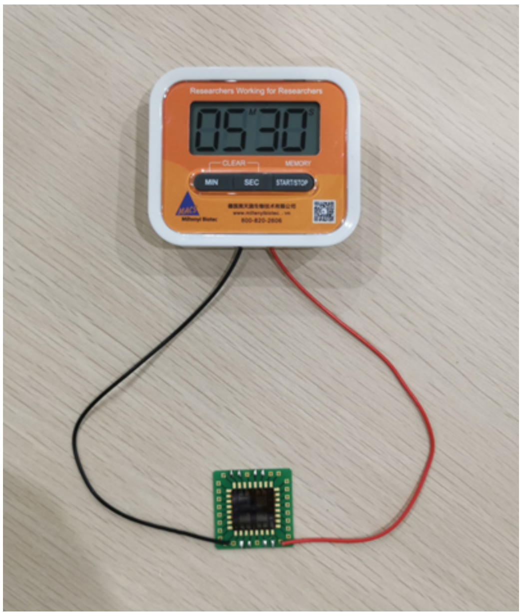


**Figure S23.** Photographs of 3D MSCs in series powering a timer.

**Table S1.** A detailed comparison of electrochemical performance of various 3D MSCs.

| **MSCs** | **Voltage** | **Capacitance** | **Cycling stability** | **Energy density** | **Ref.** |
|---|---|---|---|---|---|
| 3D LIG-N-PEDOT | 0-0.8 V | 720 μF $cm^{-2}$ (75 μA $cm^{-2}$) | 96% (10000) | NA | *Small* **2018**, *14*, 1702249[1] |
| MPG-MSCs | 0-1.0 V | 80.7 μF $cm^{-2}$ (1 V $s^{-1}$) | 98.3% (100000) | 2.5 mWh $cm^{-3}$ | *Nat. Commun.* **2013**, 4, 2487[2] |
| LPG-MPS | 0-0.9 V | 3.9 mF $cm^{-2}$ (0.3 mA $cm^{-2}$) | 93% (20000) | 0.98 mWh $cm^{-3}$ | *Nano Energy* **2016**, 26, 276-285[3] |
| B-3D-PCP | 0-1 V | 7.15 mF $cm^{-2}$ (100 mV $s^{-1}$) | 98% (30000) | 7.1 mWh $cm^{-3}$ | *Nano Energy* **2018**, 53, 182–188[4] |
| 3D LIG-MSCs | 0-0.6 V | 0.62 mF $cm^{-2}$ (5 mV $s^{-1}$) | 100% (10000) | 0.92 μWh $cm^{-2}$ | *Adv. Funct. Mater.* **2019**, *29*, 1902860[5] |
| graphene | 0-1.0 V | 0.7 mF $cm^{-2}$ (10 mV $s^{-1}$) | 77 % (11000) | 1 mWh $cm^{-3}$ | *ACS Nano* **2017**, 11, 8249-8256[6] |
| 3D CNT arrays | 0-1.0 V | 11 F $cm^{-3}$ (0.3 mA $cm^{-2}$) | 93% (10000) | 2 mWh $cm^{-3}$ | *Carbon* **2019**,155, 453-461[7] |
| 3D WJM graphene | 0-1.8 V | 5.3 mF $cm^{-2}$ (125 μA $cm^{-2}$) | 98% (10000) | 0.064 μWh $cm^{-2}$ | *Adv. Funct. Mater.* **2019**, *29*, 1807659[8] |
| EG | 0-1.0 V | 5.4 mF $cm^{-2}$ (1 mV $s^{-1}$) | 90% (5000) | NA | *Adv. Mater.* **2016**, *28*, 2217–2222[9] |
| 3D G/CNTCs | 0-1.0 V | 3.93 mF $cm^{-2}$ (100 mA $cm^{-2}$) | 98.4% (8000) | 2.42 mWh $cm^{-3}$ | *Nano Lett.* **2013**, 13, 72–78[10] |
| 3D GP | 0-1.0 V | 1.5 mF $cm^{-2}$ (10 V $s^{-1}$) | 100% (20000) | 0.38 μWh $cm^{-2}$ | *small* **2017***,* 13, 1603114[11] |
| **3D $MnO_2$ NTAs** | **0-1.0 V** | **13.2 mF $cm^{-2}$ (1.8 mA $cm^{-2}$) /16.5 F $cm^{-3}$** | **95.1% (10000)** | **1.9 μW h $cm^{-2}$ /2.38mW h $cm^{-3}$** | **This work** |

**Table S2.** Charge transfer resistance (Rct) and internal resistance (Rs) of $MnO_2$ NTAs-based MSC after different charge/discharge cycles.

| **Cycling number** | **Rs** | **Rct** |
|---|---|---|
| 1 | 149.9 Ω | 80.3 Ω |
| 2000 | 153.7 Ω | 93.4 Ω |
| 5000 | 159.9 Ω | 96.8 Ω |
| 8000 | 168.8 Ω | 101.6 Ω |
| 10000 | 178.5 Ω | 116.1 Ω |

**References**


1 W. Song, J. Zhu, B. Gan, S. Zhao, H. Wang, C. Li and J. Wang, *Small*, 2018, **14**, 1702249.

2 Z. S. Wu, K. Parvez, X. Feng and K. Müllen, *Nat. Commun.*, 2013, **4**, 2487.

3 B. Xie, Y. Wang, W. Lai, W. Lin, Z. Lin, Z. Zhang, P. Zou, Y. Xu, S. Zhou, C. Yang, F. Kang and C.-P. Wong, *Nano Energy*, 2016, **26**, 276-285.

4 C. Kim, D.-Y. Kang and J. H. Moon, *Nano Energy*, 2018, **53**, 182-188.

5 X. Shi, F. Zhou, J. Peng, R. a. Wu, Z. S. Wu and X. Bao, *Adv. Funct. Mater.*, 2019, **29**, 1902860.

6 J. Li, S. Sollami Delekta, P. Zhang, S. Yang, M. R. Lohe, X. Zhuang, X. Feng and M. Ostling, *ACS Nano*, 2017, 11, 8249-8256.

7 P. He, Z. Ding, X. Zhao, J. Liu, Q. Huang, J. Peng and L.-Z. Fan, *Carbon*, 2019, **155**, 453-461.

8 S. Bellani, E. Petroni, A. E. Del Rio Castillo, N. Curreli, B. Martín‐García, R. Oropesa‐Nuñez, M. Prato and F. Bonaccorso, *Adv. Funct. Mater.*, 2019, **29**, 1807659.

9 Z. Liu, Z. S. Wu, S. Yang, R. Dong, X. Feng and K. Mullen, *Adv. Mater.*, 2016, **28**, 2217-2222.

10 J. Lin, C. Zhang, Z. Yan, Y. Zhu, Z. Peng, R. H. Hauge, D. Natelson and J. M. Tour, *Nano Lett.*, 2013, **13**, 72-78.

11 L. Zhang, D. DeArmond, N. T. Alvarez, R. Malik, N. Oslin, C. McConnell, P. K. Adusei, Y. Y. Hsieh and V. Shanov, *Small*, 2017, **13,** 1603114.